

Supporting Information

for

Achieving Time-Dependent and Color-Tunable Ultralong Room Temperature Phosphorescence through Sodiation Reconfiguration for Dynamic 5D Information Encryption

Li Ya Liang,^a Ya Ting Gao,^a Shuai Chang,^a Jian Lv,^a Bin Bin Chen,^{*, a, b} and Da Wei Li^{*, a}

^a *Key Laboratory for Advanced Materials, Shanghai Key Laboratory of Functional Materials Chemistry, Feringa Nobel Prize Scientist Joint Research Center, Frontiers Science Center for Materiobiology & Dynamic Chemistry, School of Chemistry & Molecular Engineering, East China University of Science and Technology, Shanghai, 200237, China.*

^b *School of Science and Engineering, Shenzhen Institute of Aggregate Science and Technology, The Chinese University of Hong Kong, Shenzhen (CUHK-Shenzhen), 2001 Longxiang Boulevard, Longgang District, Shenzhen City, Guangdong 518172, China.*

^{*} *Corresponding author. E-mail: chenbinbin@cuhk.edu.cn (B.B. Chen) and daweili@ecust.edu.cn (D.W. Li).*

Materials and methods

Reagent and Apparatus. L-phenylalanine (Phe, 99%) is received from Energy Chemical Co., Ltd. Aluminum sulfate ($\text{Al}_2(\text{SO}_4)_3$, 99.99%) is purchased from Adamas-beta Reagent Co., Ltd. Sodium hydroxide (NaOH, 99%) is purchased from Aladdin Reagent Co., Ltd. All reagents are dissolved using 18.2 M Ω .cm ultrapure water. Photoluminescence (PL) spectra, phosphorescence (phos.) spectra and phos. lifetimes are determined by a FLS1000 steady state/transient fluorescence spectrometer. Absorption spectra is measured by a Lambda 950 UV-visible-near infrared spectrophotometer. Scanning electron microscopy (SEM) images can be obtained by a Helios G4 UC scanning electron microscope. Powder X-ray diffraction (XRD) spectrum is measured by an 18KW/D/max2550VB/PC rotating X-ray powder diffractometer. Fourier transform infrared (FT-IR) spectra are determined on a Nicolet6700 FT-IR spectrometer. X-ray photoelectron spectroscopy (XPS) spectra are analyzed using an ESCALAB 250Xi X-ray photoelectron spectrometer. Elemental mapping can be obtained by energy dispersive X-ray spectroscopy (EDS) used in combination with a field emission scanning electron microscope.

Synthesis process of Al/Phe-PMs. Aluminum/phenylalanine phosphorescent materials (Al/Phe-PMs) are prepared by a hydrothermal method. In detail, 0.5 mmol of Phe (0.083 g) and 4 mmol of $\text{Al}_2(\text{SO}_4)_3$ (1.369 g) are dissolved in 4.0 mL ultrapure water by ultrasonic treatment. The mixing solution is further transferred into a 10 mL screw-neck glass bottle and heated to 200 °C for 300 min. The obtained products are designated as Al/Phe-PMs for utilization. For large-scale synthesis of Al/Phe-PMs, Phe (82.6 g) and $\text{Al}_2(\text{SO}_4)_3 \cdot 18\text{H}_2\text{O}$ (2 kg) are mixed with water (4 L). Then the solution is dispensed in two 4 L beakers and heated at 200 °C for 17 h, rendering it feasible to achieve large-scale production of Al/Phe-PMs.

Synthesis of Al/Phe-PMs@NaOH. In order to prepare NaOH-treated Al/Phe-PMs (Al/Phe-PMs@NaOH), 40 mg of Al/Phe-PMs solid powder is dispersed in 1.0 M NaOH solution (2 mL) through 60 min of ultrasound. Then, Al/Phe-PMs@NaOH powder can be formed by heating the mixing solution in a vacuum drying oven at 90 °C for 15 h. To investigate the effect of the volume and concentration of NaOH solution on the phos. emission of the Al/Phe-PMs@NaOH, a series of NaOH solutions with different volumes or concentrations are used. When exploring the influence of the volume, the volume of NaOH solution (1.0 M) is 0 mL, 1 mL, 2 mL, and 3 mL, respectively. When the influence of the concentration is studied, the concentration of NaOH solution (2 mL) is expressed as 0 mM, 0.1 mM, 1 mM, 10 mM, 0.1 M, and 1.0 M, respectively.

Synthesis of Phe@NaOH. A facile thermal polymerization method is used to synthesize NaOH-treated Phe (Phe@NaOH). In detail, 40 mg of Phe is dispersed in 1.0 M NaOH solution (2 mL) through ultrasonic treatment. Next, with the treatment of heating and drying the mixed solution at 90 °C for 15 h, Phe@NaOH powder is obtained for further utilization.

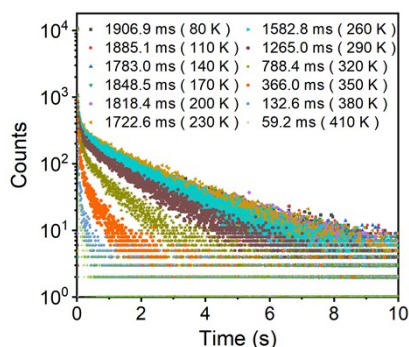


Figure S1. The phos. lifetimes of the Al/Phe-PMs at different temperatures. EX: 290 nm, EM: 540 nm. Result shows that the phos. lifetimes of the Al/Phe-PMs decrease as the temperature increases.

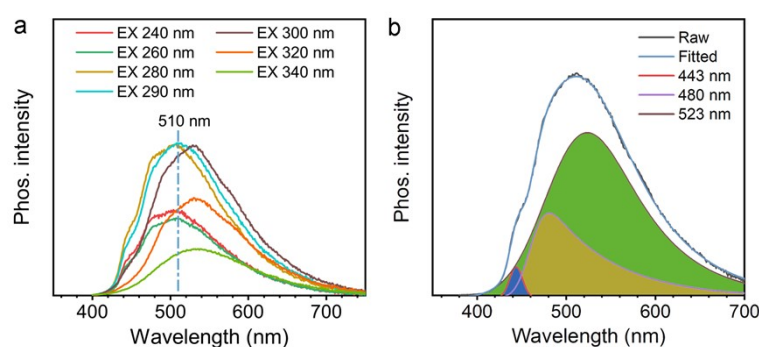


Figure S2. (a) Phos. emission spectra of Phe powder excited by different excitation wavelengths at room temperature. Result shows that Phe powder has a maximum phos. emission at about 510 nm when excited by 290 nm. (b) Peak fitting of phos. emission peak excited at 290 nm. Delay time: 5 ms.

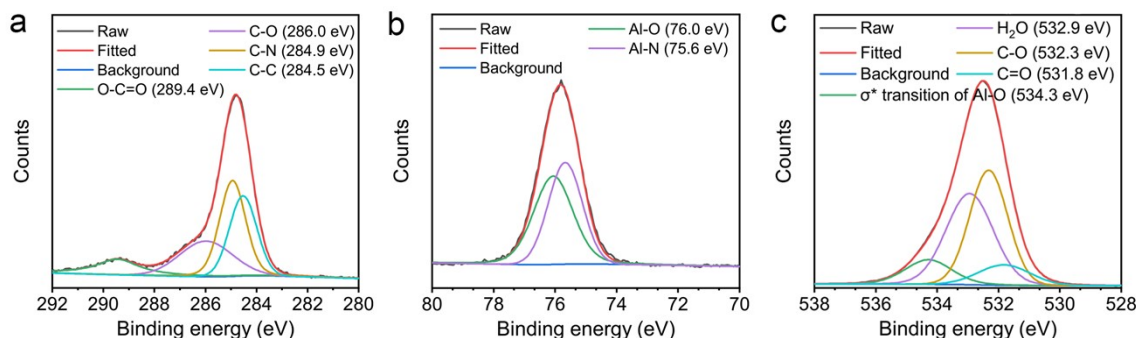


Figure S3. Structural analysis of Al/Phe-PMs. (a) High-resolution C1s spectrum, (b) high-resolution Al2p spectrum, and (c) high-resolution O1s spectrum of Al/Phe-PMs. Results show that many carboxylate groups exist in Al/Phe-PMs due to the characteristic binding energy of 289.4 eV in high-resolution C1s spectrum. High-resolution Al2p spectrum further reveals that Al³⁺ ions not only coordinate with carboxyl groups through Al–O bonds, but can also coordinate with amino groups through Al–N bonds. Moreover, a typical peak located at 534.3 eV corresponding to the σ^* transition of Al–O bond is found in high-resolution O1s spectrum.

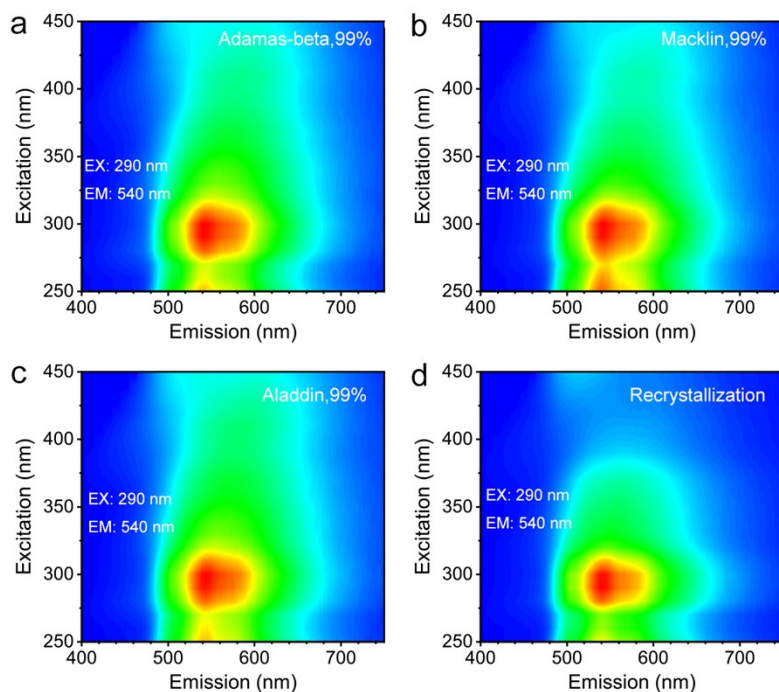


Figure S4. 3D phos. spectra of the Al/Phe-PMs prepared using (a-c) Phe ligands with a purity of 99% from different manufacturers and (d) recrystallized Phe ligands. Results show that there is no significant difference in the phos. spectra of the prepared Al/Phe-PMs, whether using Phe from different manufacturers or recrystallized Phe. Delay time: 5 ms.

Table S1. The comparison of phos. efficiency of common RTP materials. $\phi_{\text{Phos.}}$ refers to the phos. QYs. $\tau_{\text{Phos.}}$ refers to the phos. lifetime.

RTP materials	$\phi_{\text{Phos.}}$ (%)	$\tau_{\text{Phos.}}$ (s)	Ref.
TSP crystals	66.9	0.17	1
CDs-4	47.0	0.63	2
syn-BTCz-doped PVA films	29.8	0.85	3
IbCzA-doped PVA film	19.8	1.81	4
TMA	18.2	0.16	5
Py-BOH-PVA	13.1	0.34	6
CNQDs	10.5	6.47	7
Phe9-B-R	9.4	2.67	8
CT5-0	9.3	1.13	9
DPCz-doped PVA	0.3	1.94	10
Al/Phe-PMs	7.98	1.0153	This work

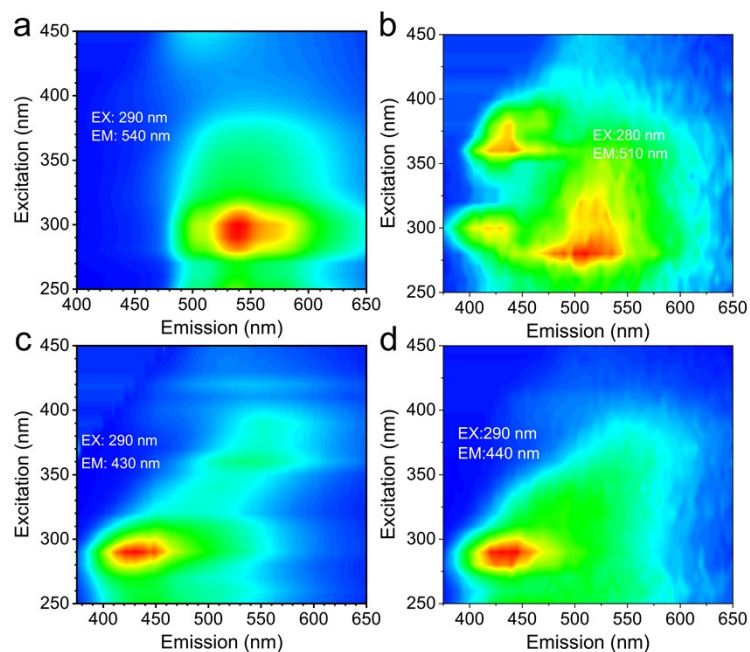


Figure S5. The 3D phos. spectra of Al/Phe-PMs@NaOH prepared by using different volumes of 1.0 M NaOH (from a to d: 0 mL, 1 mL, 2 mL, and 3 mL). Results show that the phos. emission of the material gradually blueshifts with the increase of the NaOH volume, and reaches a plateau at the volume of 2 mL. Delay time: 5 ms.

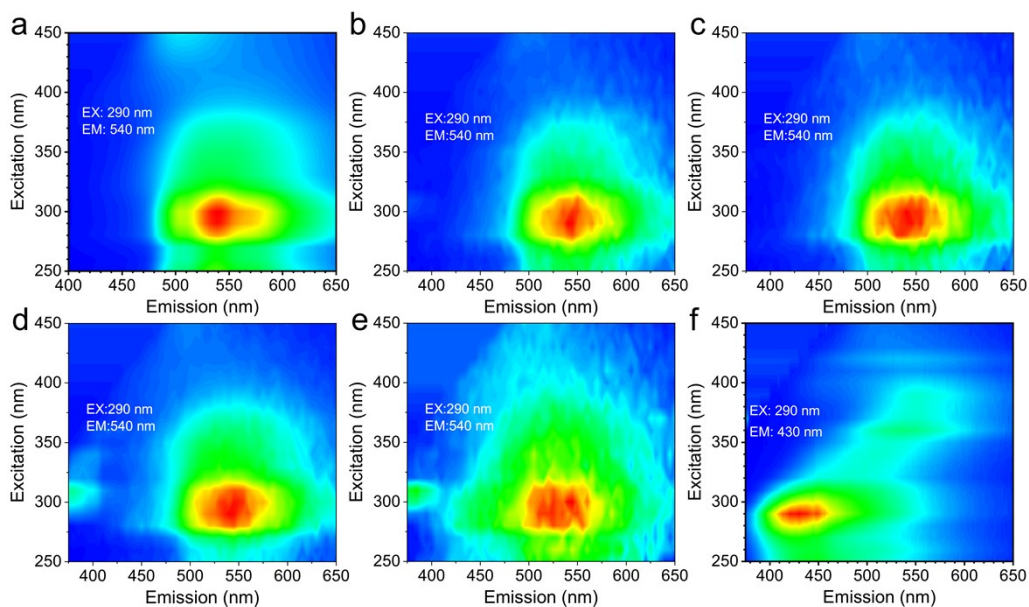


Figure S6. The 3D phos. spectra of Al/Phe-PMs@NaOH prepared by using different concentrations of NaOH (from a to f: control, 0.1 mM, 1 mM, 0.01 M, 0.1 M, and 1.0 M). Results show that the phos. emission of the material blueshifts to 430 nm when the concentration of NaOH is 1.0 M. Volume: 2 mL. Delay time: 5 ms.

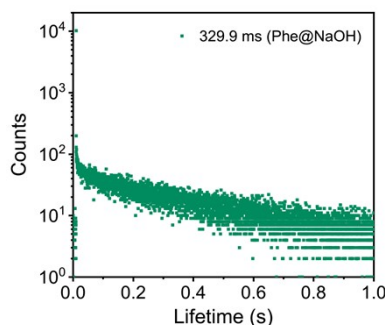


Figure S7. Phos. lifetime of Phe@NaOH at room temperature. Result shows that the phos. lifetime of Phe@NaOH is close to that of Al/Phe-PMs@NaOH.

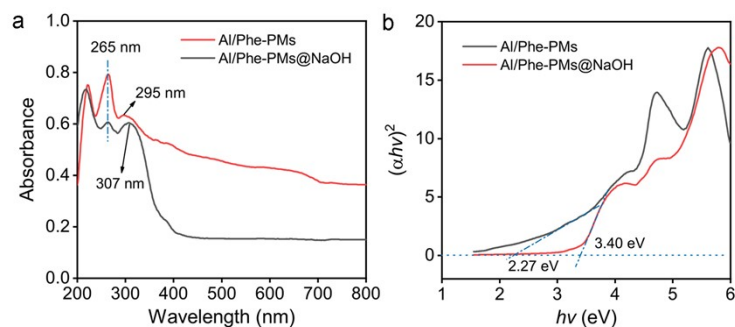


Figure S8. (a) Absorption spectra and (b) the $(\alpha hv)^2 - hv$ curves of Al/Phe-PMs and Al/Phe-PMs@NaOH. Results show that Al/Phe-PMs have a stronger and wider absorption band from 400 to 800 nm as compared to Al/Phe-PMs@NaOH, indicates the destruction of rigid configuration caused by NaOH, accompanied by an increase in optical bandgap from 2.27 eV to 3.40 eV.

Table S2. The photophysical rate constants of Al/Phe-PMs before and after the treatment of NaOH.

	$\phi_{\text{Phos.}}$ (%)	$\tau_{\text{Phos.}}$ (ms)	k_r (s^{-1})	k_{nr} (s^{-1})
Al/Phe-PMs	7.98	1015.3	7.86×10^{-2}	0.91
Al/Phe-PMs@NaOH	1.22	393.1	3.10×10^{-2}	2.51

The phos. radiative rate constant of Al/Phe-PMs is calculated according to the following equation:

$$k_r = \phi_{\text{Phos.}} / \tau_{\text{Phos.}} \quad (1)$$

Moreover, the non-radiative rate constant of Al/Phe-PMs is calculated based on the following equation:

$$k_{\text{nr}} = (1 - \phi_{\text{Phos.}}) / \tau_{\text{Phos.}} \quad (2)$$

Wherein, $\phi_{\text{Phos.}}$ refers to the phos. QYs. $\tau_{\text{Phos.}}$ refers to the phos. lifetime. k_r refers to the phos. radiative rate constant. k_{nr} refers to the non-radiative rate constant.

Reference:

1. W. Ye, H. Ma, H. Shi, H. Wang, A. Lv, L. Bian, M. Zhang, C. Ma, K. Ling, M. Gu, Y. Mao, X. Yao, C. Gao, K. Shen, W. Jia, J. Zhi, S. Cai, Z. Song, J. Li, Y. Zhang, S. Lu, K. Liu, C. Dong, Q. Wang, Y. Zhou, W. Yao, Y. Zhang, H. Zhang, Z. Zhang, X. Hang, Z. An, X. Liu and W. Huang, *Nat. Mater.*, 2021, **20**, 1539-1544.
2. X. Liu, W. Liu, K. Zuo, J. Zheng, M. Wang and X. Liu, *ACS Sustainable Chem. Eng.*, 2023, **11**, 1809-1819.
3. Y. Xie, Z. Wang, P. Yu, L. Zhang, Y. Geng and J. Zhao, *Adv. Optical Mater.*, 2023, DOI: 10.1002/adom.202301188.
4. Y. Yang, Y. Liang, Y. Zheng, J. A. Li, S. Wu, H. Zhang, T. Huang, S. Luo, C. Liu, G. Shi, F. Sun, Z. Chi and B. Xu, *Angew. Chem. Int. Ed.*, 2022, **61**, e202201820.
5. H. Liu, W. Ye, Y. Mu, H. Ma, A. Lv, S. Han, H. Shi, J. Li, Z. An, G. Wang and W. Huang, *Adv. Mater.*, 2022, **34**, 2107612.
6. D. Li, J. Yang, M. M. Fang, B. Z. Tang and Z. Li, *Sci Adv*, 2022, **8**, eabl8392.
7. B. Han, X. Lei, D. Li, Q. Liu, Y. Chen, J. Wang and G. He, *Adv. Optical Mater.*, 2023, **11**, 2202293.
8. Q. Gao, M. Shi, M. Chen, X. Hao, G. Chen, J. Bian, B. Lü, J. Ren and F. Peng, *Small*, 2023, DOI: 10.1002/sml.202309131.
9. S. Xu, W. Wang, H. Li, J. Zhang, R. Chen, S. Wang, C. Zheng, G. Xing, C. Song and W. Huang, *Nat. Commun.*, 2020, **11**, 4802.
10. Y. Zhang, Y. Su, H. Wu, Z. Wang, C. Wang, Y. Zheng, X. Zheng, L. Gao, Q. Zhou, Y. Yang, X. Chen, C. Yang and Y. Zhao, *J. Am. Chem. Soc.*, 2021, **143**, 13675-13685.